Accepted Manuscript

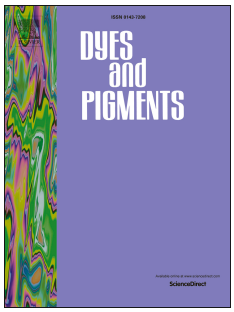

A pH-responsive organic photosensitizer specifically activated by cancer lysosomes

Fengfeng Xue, Peng Wei, Xiaoting Ge, Yaping Zhong, Chunyan Cao, Danping Yu, Tao Yi

PII: S0143-7208(18)30451-0

DOI: 10.1016/j.dyepig.2018.04.008

Reference: DYPI 6669

To appear in: *Dyes and Pigments*

Received Date: 27 February 2018

Revised Date: 5 April 2018

Accepted Date: 6 April 2018

Please cite this article as: Xue F, Wei P, Ge X, Zhong Y, Cao C, Yu D, Yi T, A pH-responsive organic photosensitizer specifically activated by cancer lysosomes, *Dyes and Pigments* (2018), doi: 10.1016/j.dyepig.2018.04.008.

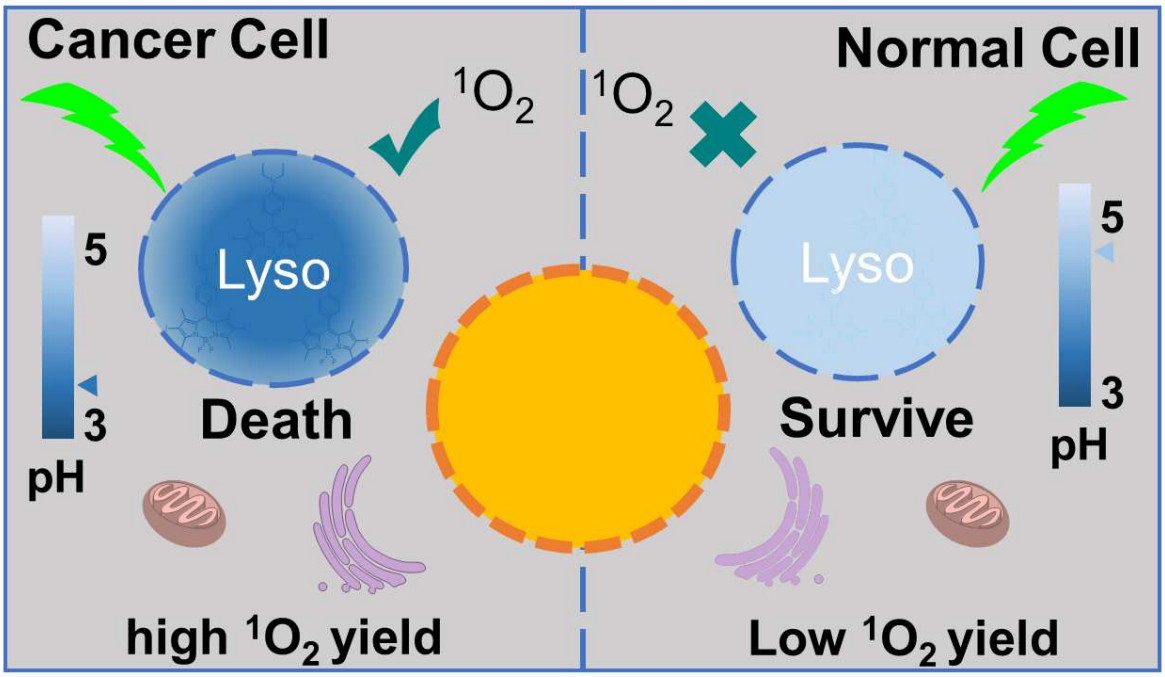

A pH-responsive organic photosensitizer specifically activated by cancer lysosomes

Fengfeng Xue,[a] Peng Wei,[a] Xiaoting Ge,[b] Yaping Zhong,[a] Chunyan Cao,[a] Danping Yu,[a] Tao Yi*[a]

a Department of Chemistry and Collaborative Innovation Center of Chemistry for Energy Materials, Fudan University, Shanghai 200433, China

b College of Science and Hebei Research Center of Pharmaceutical and Chemical Engineering, Hebei University of Science and Technology, Yuhua Road 70, Shijiazhuang 050080, PR China

Keywords

BODIPY, pH responsive, lysosome, photodynamic therapy

Highlight

1. **pH-PDT** is highly sensitive to pH in the range of 5.5-3.0 with increased emission at 555 nm for about 12-fold

2. **pH-PDT** shows increased singlet oxygen quantum yield from 0.24 to 0.45 when pH decreases from 5.5 and 3.5

3. **pH-PDT** locates in lysosomes of cancer cell for photodynamic therapy of cancer and have no obvious toxicity of normal cells

Abstract

Photodynamic therapy that can cause high toxicity in cancer cells and lower toxicity in normal cells is in great demand. Herein, we report a pH-responsive photosensitizer based on BODIPY (**pH-PDT**) by specific response to lysosomes of cancer cells for efficient photo dynamic therapy. The photosensitizer is highly sensitive in the pH range of 5.5-3.0, exhibiting an increased emission at 555 nm for about 12-fold. *In vitro* experiments confirmed that the singlet oxygen quantum yield of the photosensitizer was increased from 0.24 to 0.45 in an acidic environment (pH 5.5 to 3.5). With different pH of lysosomes in cancer cells and normal cells, the **pH-PDT** can specifically respond to lysosomes of cancer cell (HePG-2 cell) for photodynamic therapy of cancer and have no obvious toxicity of normal cells (HL-7702 cells).

Introduction

Photodynamic therapy (PDT), in which the energy of light can be transformed to $^3O_2$ to generate singlet oxygen by irradiating a photosensitizer (PS) with light at certain wavelengths, has been recognized as one of the most efficient treatment modalities for cancer, owing to its high specificity and minimal invasiveness.[1-3] However, the inevitable side effects of PDT have limited its extensive clinical use to date.[4] Although drug delivery nanoparticles have been well-developed for efficient cancer therapy, only 0.7% (median) of the administered nanoparticle dose is delivered to the solid tumour.[5] This means that more than 90% of the toxic drugs are absorbed by normal organs and cells,

which is the main reason for undesirable side effects in cancer therapy. Generally, the patients treated with PDT must refrain from sunlight or other forms of light exposure for at least 30 days, because most of the administered PSs are retained by normal cells.[6] Therefore, development of stimulating responsive PSs that can be activated by specific cancer cell environments while limiting toxicity to normal cells, is in great demand.

Various stimulating responsive PSs that can be activated by the stimulus of enzymes[7,8], DNA[9,10], heat[11], and small molecules[12-14] to enhance the efficiency and precision of PDT, have been reported. However, those stimulating responsive PSs generally could not distinguish between normal and cancer cells. Due to the high invasiveness and permeability of cancer cells, their organelle microenvironment is different from normal cells, which may be exploited for the development of a stimulating responsive PS.[15,16]

It is well-known that lysosomes play a key role in cellular processes. They can receive and degrade unwanted materials from outside of the cell and obsolete components inside the cell with the aid of numerous acid hydrolases.[17] To maintain the optimal activity of hydrolases, lysosomes dwell in the acidic microenvironment because of the proton-pumping vacuolar ATPase.[15,16] Various pH-responsive PSs that can be activated by the acidic lysosome environment have been reported. For example, O'Shea first reported an iodinated BODIPY with attaching photo induced electron transfer (PET)-based quenchers for pH-activated PDT.[17] Huangxian Ju and colleagues have reported

lysosome-targeted and pH-controlled nanoparticles, on which folate was covalently-linked to recognize cancer cells for enhanced PDT.[18] However, a PS that is stimulated only by cancer cell lysosome and remains silent in normal cells without complex target molecules, has not yet been reported. Compared with normal cells, the lysosomal pH (pH_{lys}) in cancer cells (pH_{lys} 3.8–4.7) shows a higher acidity than that in normal cells (pH_{lys} 4.5–6.0), mainly owing to the increased expression of specific subunits that promote the pumped efficiency of H^+ by V-ATPase.[19-22] These lysosome pH differences between normal and cancer cells may be used as a strategy to design a responsive PS. However, it is challenging to find lysosome targeted PS with a smart pKa of 3.8–4.5 for efficient photodynamic therapy (PDT) only in cancer cells.

BODIPY (4,4-Difluoro-4-bora-3a,4a-diaza-s-indacene) derivatives are one kind of commonly used fluorescent dye for ion sensors and imaging probes.[23,24] Actually, BODIPYs have many ideal PS characteristics such as high extinction coefficients, resistance to photobleaching, and higher light–dark toxicity ratios.[25,26] However, only a few of the derivatives have been designed for PDT application.[1,27]

To distinguish lysosomes of cancer cells and normal cells, a smart pH responsibility with suitable pKa is requirement. Amino modified BODIPYs generally show pH sensitivity. For example, Urano et al. has recently reported a N,N-diethylaminophenyl (4-position) modified 2,6-dicarboxyethyl-1,3,5,7-tetramethyl-BODIPY (DiEtNBDP) with a pKa of

6.0 as a pH-responsive fluorescent marker for lysosome imaging.[28] However, the pH sensitivity of this molecule is not enough to distinguish between normal and cancer cells. Herein, by substituting carboxyethyl for iodine of 2,6-position of DiEtNBDP, we report a novel pH-responsive PS (**pH-PDT** in Figure 1a), which can preferentially be activated by lysosomes of cancer cells via concentration control. While introduction of iodine can endow the **pH-PDT** with a photodynamic effect, the iodine that behaves as a weak electron-donating group successfully lowers the pKa of DiEtBDP from 6.0 to 4.0. With the N,N-diethylaminophenyl group in 4-position, **pH-PDT** can not only be specifically accumulated in lysosomes, but also be highly responsive to pH in the range of 3.0–5.0 (the leap point at pH 4.5). In the more acidic microenvironment, **pH-PDT** exhibited stronger emission at 555 nm and increased production of singlet oxygen. Consequently, **pH-PDT** can act as a smart PS that shows much more efficient photodynamic action for cancer cells than for normal cells in enhanced PDT of cancer.

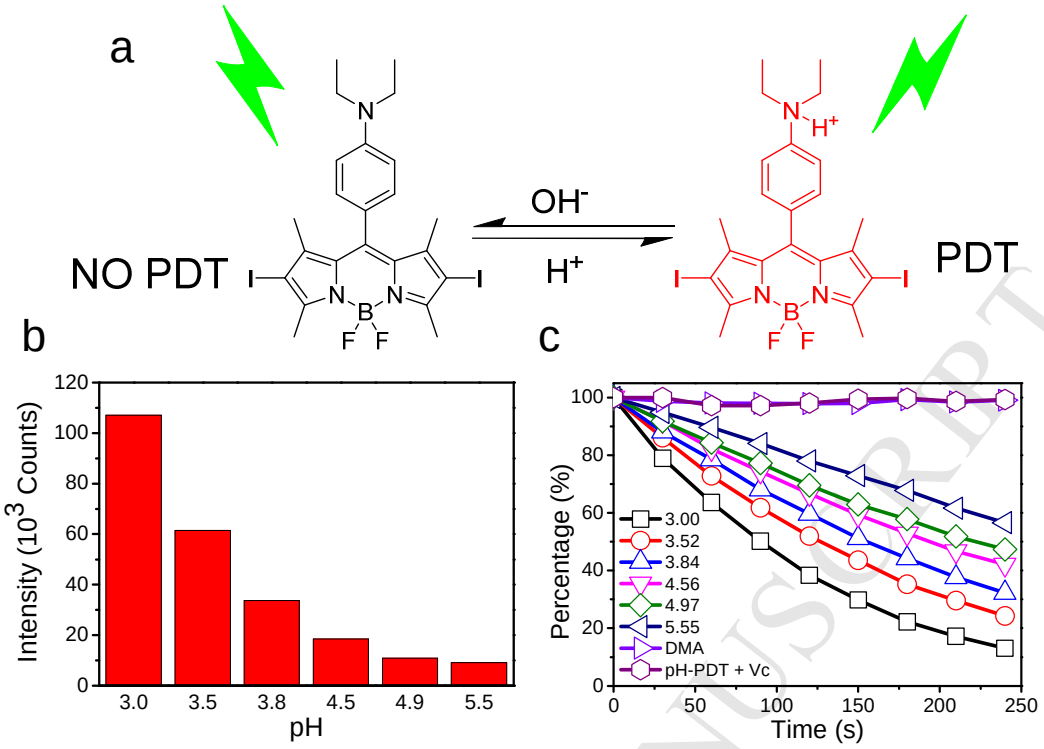

Fig. 1. a) Illustration of pH-responsive **pH-PDT**, b) fluorescent intensity changes of **pH-PDT** (10 μM) at 555 nm in different pH value (3.0, 3.5, 3.8, 4.5, 4.9 and 5.5), c) decay profiles of the emission of DMA (50 μM) at 400 nm without **pH-PDT**, in the presence of **pH-PDT** (10 μM) with different pH in PBS, and **pH-PDT** with Vc (100 μM), irradiated by 532 nm laser (50 mW/cm^2).

Results and discussion

The photo-physical properties of **pH-PDT** were measured in phosphate-buffered saline (PBS) (Table S1). The pH-responsiveness of **pH-PDT** was evaluated from pH 3.0 to 5.5 in PBS using fluorescent spectroscopy. **pH-PDT** exhibited moderate emission at 553 nm (fluorescent quantum yield, 0.012) only in acidic conditions owing to the protonation of diethylamino (Figure 1b). When the pH value was increased, the emission at

553 nm was decreased by a factor of 12 from pH 3.0 to 5.5 (pKa = 4.0). In neutral and alkaline conditions, **pH-PDT** showed minimal fluorescence because of the PET effect. The absorption of **pH-PDT** from 450 to 600 nm showed no obvious change with pH, further confirming the PET effect of **pH-PDT** (Figure S1). The photostability of **pH-PDT** was measured by exposing it to 532 nm laser (50 mW/cm^2) (Figure S2). **pH-PDT** was destroyed less than 5% of the time when irradiated by laser for 20 min, indicating its excellent stability.

To investigate the pH-dependent photodynamic behaviour of **pH-PDT**, 9,10-dimethylanthracene (DMA), which is recognized as a singlet oxygen indicator, was used to monitor the production of singlet oxygen. As shown in Figure 1c, upon addition of **pH-PDT** to the solution, the emission of DMA decreased significantly at a wavelength of 400 nm over 240 s under 532 nm laser irradiation (50 mW/cm^2). For comparison, the emission of DMA never decreased due to addition of Vitamin C (Vc, an inhibitor of singlet oxygen). More importantly, **pH-PDT** in different pH conditions exhibited a variable singlet oxygen production ability. In the presence of **pH-PDT**, the emission of DMA at 400 nm was decreased to 13.02%, 24.26%, 32.25%, 42.11%, 47.33%, and 56.60%, irradiated by 532 nm laser for 240 s at the pH of 3.00, 3.52, 3.84, 4.56, 4.97, and 5.55, respectively (Figure 1c). The singlet oxygen quantum yield of **pH-PDT** at a pH of 3.5 and 5.5 was 0.45 and 0.24, respectively (Ce6 in

DMSO as standard), indicating a more efficient singlet oxygen production of **pH-PDT** in more acidic conditions.

With consideration to the pH-controlled photodynamic property of **pH-PDT** in solution, *ex vivo* experiments were conducted. The toxicity of **pH-PDT** toward normal and tumour cells was first valuated using the MTT method. As shown in Figure S2, **pH-PDT** showed little or no cytotoxicity (> 90% viability) in both normal (HL-7702) and tumour cells (HePG-2), indicating that **pH-PDT** can be used as a proper PS candidate for PDT.

To determine the precise distribution of **pH-PDT** in cancer (HePG-2) and normal (HL-7702) cells, co-localization experiments in lysosomes were conducted. Cells loaded with **pH-PDT** were incubated with the commercial dye Lyso Tracker red. As shown in Figure 2, **pH-PDT** accumulated in the lysosomes in both HePG-2 and HL-7702 cells. The merged images and correlation analysis images show that the green (from **pH-PDT**) and red (from Lyso Tracker Red) fluorescence were well overlapped, indicating precise lysosome **pH-PDT** accumulation. The Pearson's correlation coefficient in HePG-2 and HL-7702 cell were 0.85 and 0.74, respectively.

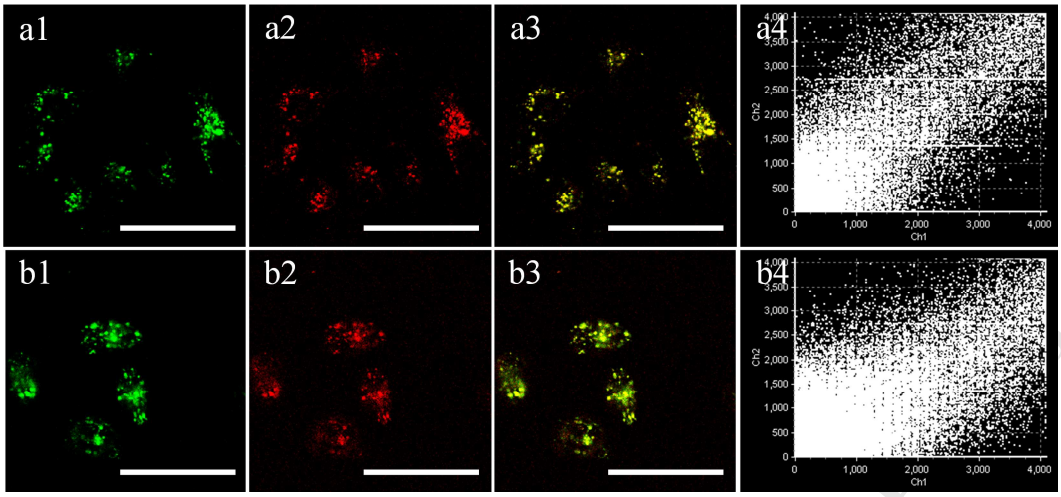

Fig. 2. CLSM images of HePG-2 (a) and HL-7702 (b) cells co-labelled with **pH-PDT** (1) /Lyso tracker red (2). Green channel (1): 550 ± 25 nm for **pH-PDT** (5 μM), λex = 488 nm; Red channel (2): 650 ± 25 nm for Lyso tracker red (200 nM), λex = 543 nm; Merged images (3); correlation analysis images (4); scale bar: 50 μm.

PDT experiments were then carried out in HePG-2 and HL-7702 cells to compare the PDT efficiency between tumour and normal cells. Cells were incubated with **pH-PDT** for 30 min, washed with culture medium, irradiated with 532 nm laser light (10 mW/cm^2) for 0–4 min, and incubated for a further 24 h. It was surprised that the PDT efficiency of **pH-PDT** in normal and cancer cells could be precisely controlled by changing the concentration of **pH-PDT** and laser power density. When the concentration of **pH-PDT** was 1 μM and the power density was 10 mW/cm^2, the difference in cell toxicity (Δ) between HL-7702 and HePG-2 cells was obvious, as shown in Figure S4. With a higher concentration of **pH-PDT**, e.g. ≥ 2 μM, cell cytotoxicity in both normal and cancer cells was apparent after irradiating with 532 nm laser for more than 1 min, even though normal cell viability is higher than that of cancer cells.

Therefore, 1 μM of **pH-PDT** and 10 mW/cm^2 of laser power was selected as the optimal condition for the follow-up PDT experiments. As demonstrated in Figure 3b-3d, the cell viability of normal cells (> 90%) was unchanged after **pH-PDT** treatment compared with the control (C), laser only (L), or **pH-PDT** without irradiation (0) groups. However, cell viability of cancer cells was dramatically decreased after extended irradiation. Prolonging incubation time after PDT treatment would further decrease cell viability only for cancer cells. These results indicate that **pH-PDT** can enable killing of cancer cells with 532 nm laser irradiation but has less effect on normal cells.

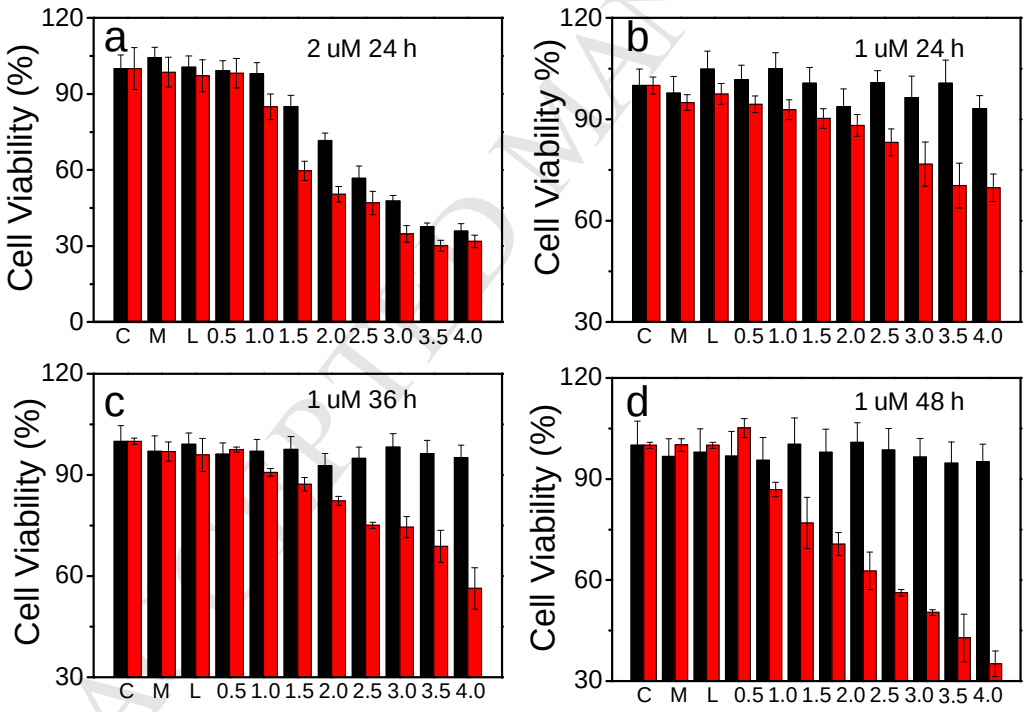

Fig. 3. PDT of cancer (red) and normal cells (black). Cells were treated with **pH-PDT** (2 μM for a, 1 μM for b, c, d) irradiated by 532 nm laser (10 mW/cm^2), the experiment was divided into seven groups: Control (C), laser only (L), **pH-PDT** without irradiation (M) and irradiated with laser for 0.5, 1.0, 1.5, 2.0, 2.5, 3.0, 3.5, 4.0

min, then cells were incubated for further 24 h (a), 24 h (b), 36 h (c), 48 h (d).

To confirm the generation of singlet oxygen in living cells, the singlet oxygen sensor green (SOSG) was used. As shown in Figure 4, only cancer cells (HePG-2 cells) were stained green. Both of the cell types in the presence of Vc showed no emission. This indicated that the singlet oxygen was only generated in cancer cells and that PDT was specific due to the lower pH value of lysosomes in cancer cells than in normal cells.

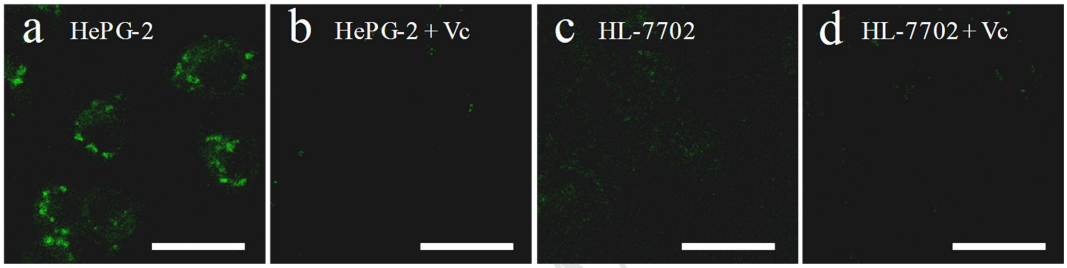

Fig. 4. Confocal fluorescent images of HepG-2 cells and HL-7702 cells with treatment of **pH-PDT** (1 μM) after 532 nm irradiation stained by SOSG, HePG-2 cells without Vc for a, HePG-2 cells with Vc for b, HL-7702 cells without Vc for c, HL-7702 cells with Vc for d, 515 ± 25 nm for SOSG (5 μg/mL), λex = 488 nm, scale bar: 50 μm.

The differential PDT effects were further confirmed by co-staining of cells with Calcein AM (AM, specifically staining live cells green) and propidium iodide (PI, specifically staining dead cells red). As shown in Figure 5, HL-7702 cells were in good condition, only showing green fluorescence after 532 nm irradiation, indicating that **pH-PDT** had minimal photodynamic toxicity on normal cells. In contrast, obvious cell death occurred in HePG-2 cells (marked by red fluorescence) after 532 nm laser irradiation. These results further

confirmed that PDT with **pH-PDT** was specifically activated by the acidic microenvironment of cancer cells.

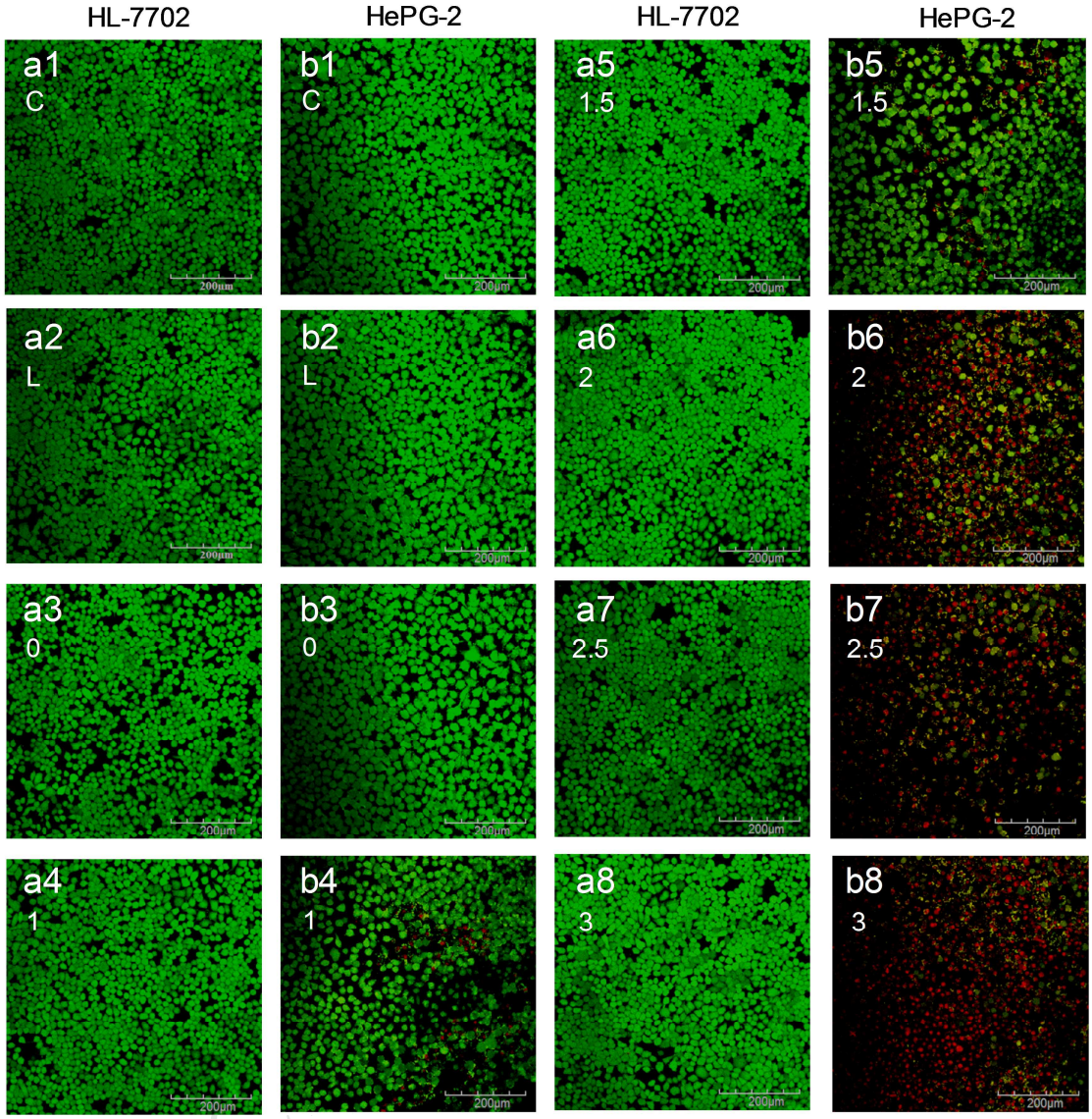

Fig. 5. CLSM images of Calcein Am/PI stained HL-7702 (a) and HePG-2 (b) cells with or without **pH-PDT** (1 μM) treated after exposed to 532 nm laser (10 mW/cm^2) at different times. The experiment was divided into eight groups: Control (1), only laser (2), **pH-PDT** without irradiation (3) and **pH-PDT** irradiated with laser for 1 (4), 1.5 (5), 2 (6), 2.5 (7) and 3 (8) min. Red channel: 617 ± 25 nm for PI (200 nM), λex = 543 nm; green channel: 515 ± 25 nm for AM (200 nM), λex = 488 nm, scale bar: 200

μm.

Conclusions

In conclusion, we have developed a lysosome-targeted and pH-sensitive photosensitizer, **pH-PDT**, for PDT. The designed BODIPY-based pH-sensitive agent can accept a proton to increase its fluorescent intensity and ability of singlet oxygen production. Due to the differences in pH levels of normal and cancer cell lysosomes, **pH-PDT** can be specifically activated by cancer cell lysosomes for PDT and have minimal toxicity in normal cells. This work provides an efficient strategy to design smart drugs for superior PDT efficacy.

Experimental

1.1 Materials and characterization

All the starting materials were obtained from commercial suppliers and used as received. 2,4-dimethylpyrrole, 4-diethylaminobenzaldehyde, $BF_3{\cdot}H_2O$, Et_3N were purchased from J&K Chemical Technology. N-iodosuccinimide and trifluoroacetic acid were purchased from Energy Chemical Company. 2,3-Dicyano-5,6-dichlorobenzoquinone was purchased from Beijing InnoChem Science & Technology Co., Ltd. All organic solvents were supplied from Strong Chemical Company (Shanghai, China). Singlet oxygen green sensor

(SOSG), MTT, Calcien AM (AM), propidium iodide (PI) and cell culture reagents were purchased from Invitrogen.

1.2 Instruments

^{1}H NMR and ^{13}C NMR spectra were recorded with a Bruker DRX 500 spectrometer at 400 and 100 MHz, respectively. Proton chemical shifts are reported in parts per million downfield from tetramethylsilane (TMS). The high-resolution mass spectra (HR-MS) were measured on a Bruker Micro TOF II 10257 instrument. UV-visible spectra were recorded on a Shimadzu UV-2550 spectrometer. Steady emission experiments at room temperature were measured on an Edinburgh instrument FLS-920 spectrometer with a Xe lamp as an excitation source. The quantum yield and lifetime were measured by QM40. Confocal laser scanning microscopy (CLSM) was performed on an Olympus FV1000 confocal fluorescence microscope with a 60× oil-immersion objective lens.

1.3 Synthesis

The Synthetic process of **pH-PDT** is shown in Scheme 2.

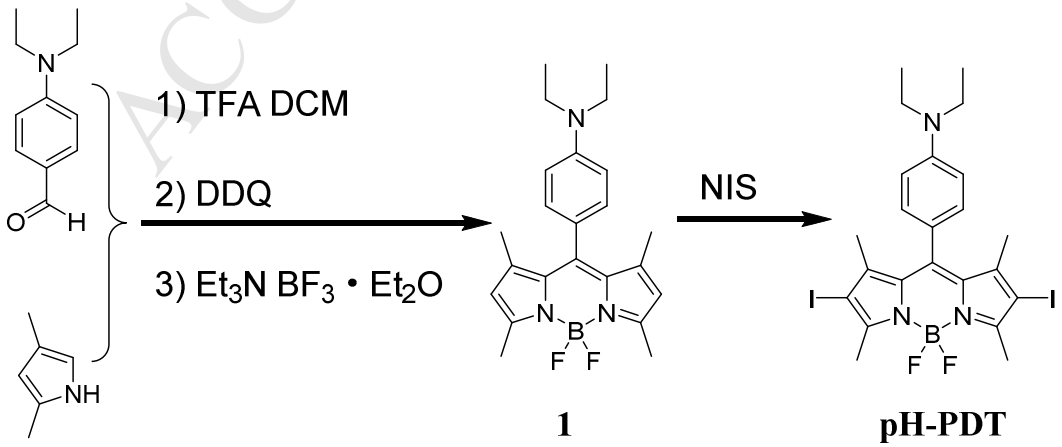

Scheme 2. The synthesis route of pH-PDT.

Under N_2 atmosphere, 2,4-dimethylpyrrole (0.95 g) and 4-diethylaminobenzaldehyde (1 g) in dry CH_2Cl_2 (250 mL) was stirred at r.t. On cooling with an ice bath, TFA (0.1 mL) was added via syringe, and the mixture was stirred overnight at r.t. A solution of DDQ (1.22 g) in THF (30 mL) was added via addition funnel, and the mixture was stirred at r.t. for 7 h. Triethylamine (4.2 mL) was added dropwise with cooling on an ice bath, and the mixture was stirred for another 0.5 h. Then, $BF_3{\cdot}Et_2O$ (5.26 mL) was added dropwise with a syringe, and the reaction mixture was stirred overnight. The solution was concentrated under reduced pressure, and water (200 mL) was added. The mixture was stirred for 24 h and extracted with CH_2Cl_2. The organic layer was dried over anhydrous Na_2SO_4, and the solvent was evaporated under reduced pressure. The crude product was purified by column chromatography (silica gel, CH_2Cl_2/hexane 1:1, v/v) to give **1** as green solid. Yield 200 mg 16.0%. ^{1}H NMR (400 MHz, $CDCl_3$): 7.00 (2H, d), 6.72 (2H, d), 5.96 (2H, s), 3.39 (4H, dd), 2.54 (6H, s), 1.51 (6H, s) 1.19 (6H, t), ^{13}C NMR (100 MHz, $CDCl_3$): 154.65, 148.32, 143.24, 129.01, 120.81, 112.12, 44.39, 30.45, 30.26, 29.70, 14.64, 14.51, 12.37. HR-MS (ESI Positive) calc. for $C_{23}H_{29}BF_2N_3^+$, 396.2417 [M^+], found 396.2403.

1 (200 mg) and N-iodosuccinimide (NIS, 468 mg) were dissolved in dry CH_2Cl_2 (50 mL). The mixture was stirred at room temperature. Then, the precipitate was collected to give **pH-PDT** as a red solid. Yield 300 mg 89%. ^{1}H

NMR (400 MHz, $CDCl_3$): 6.96 (2H, d), 6.75 (2H, d), 3.43 (4H, dd), 2.64 (6H, s), 1.54 (6H, s) 1.21 (6H, t), ^{13}C NMR (100 MHz, $CDCl_3$): 155.84, 148.60, 145.43, 132.17, 129.24, 128.97, 120.68, 112.01, 85.16, 44.40, 17.36, 15.94, 12.35. for $C_{23}H_{27}BF_2N_3I_2^+$, 648.0350 [M^+], found 648.0360.

1.4 Quantum yields of singlet oxygen

PBS/ethanol (v:v 2:1) solution (3 mL) containing **pH-PDT** at pH 3.5 and 5.5 was put in a quartz cuvette with an optical path length of 1.0 cm. The cuvette was illuminated by 532 nm laser (GG-532-1500 MW) with a power density of 50 mW/cm^2 for every 30 seconds. The decrease of DMA at 400 nm was monitored by fluorescent spectra. The singlet oxygen quantum yields of pH-PDT was determined according to previous method as following equation.

$$\phi_\Delta = \frac{r / A}{r_s / A_s} * \phi_{\Delta s}$$

Where φ_Δ is the singlet oxygen quantum yields, r and r_s are the reaction rate of DMA with singlet oxygen generated from photosensitization of **pH-PDT** and Ce6, respectively. A and A_s are the absorbance of **pH-PDT** and Ce6, respectively, and $\varphi_{\Delta s}$ (0.53) is the singlet oxygen quantum yields of Ce6.

1.5 Cell culture

The cancer cells (HePG-2) and normal cells (HL-7702) were provided by the Institute of Biochemistry SIBS, CAS (China) and Cell Biology and Wuhan Procell life science & Technology Co. Ltd. Cells were cultured in phenol-red-free Dulbecco's modified essential medium (RPMI 1640) supplemented with 10% fetal bovine serum (FBS) and 1% Pen-Strep. Cells

were incubated at 37 °C under 5% CO_2 and split with trypsin/EDTA solution (0.25%) as recommended by the manufacturer.

1.6 CLSM Imaging

HePG-2 and HL-7702 cells (5×10^8 /L) were plated on 14 mm glass coverslips and allowed to adhere for 24 h. Then the cells were incubated with pH-PDT (5 μM) for 2 h at 37 °C. The pH-PDT loaded cells were incubated with commercial dyes Lyso Tracker Red (200 nM) for 30 min. After incubation, the cells were washed three times with PBS. CLSM imaging was performed on an Olympus FV1000 confocal scanning system with a 60× oil-immersion objective lens. Green channel: 550 ± 25 nm for pH-PDT (5 μM), λex = 488 nm; Red channel: 650 ± 25 nm for Lyso tracker (200 nM), λex = 543 nm.

The detection of singlet oxygen in live cells: The experiment was divided into eight groups: Control (C), laser only (L), pH-PDT without laser (0), and with laser for 1.0, 1.5, 2.0, 2.5 and 3.0 min. HePG-2 and HL-7702 cells (5×10^8 /L) were plated on 14 mm glass coverslips and allowed to adhere for 24 h. Then the cells were incubated with pH-PDT (1 μM) and singlet oxygen sensor green (5 μg/mL) for 2 h at 37 °C, washed with cell culture medium. After that, cells were exposed to 532 nm laser (10 W/cm2) for 1.0, 1.5, 2.0, 2.5 and 3.0 min and incubated for another 48 h. CLSM imaging was performed on an Olympus FV1000 confocal scanning system with a 60× oil-immersion objective lens. Green channel: 515 ± 25 nm for singlet oxygen sensor green, λex = 488 nm;

1.7 MTT assay

The methyl thiazolyl tetrazolium (MTT) assay was used to detect the cytotoxicity of **pH-PDT**. Cells were seeded in 96-well plates at a density of 1×10^4 cells per well, then cultured in 5% CO_2 at 37 °C for 24 h. After the cells were incubated with **pH-PDT** at different concentrations (0, 0.25, 0.5, 1, 1.25, 2.5, 5, 10, 12.5 and 25 μM) in PBS for 12 and 24 h, respectively. MTT (20 μL, 5 mg/mL) was added to each well of the 96-well assay plate for 4 h at 37°C. After dimethyl sulfoxide (DMSO, 200 mL/well) was added, the absorbance was measured at 490 nm using a microplate reader. All samples were analysed in triplicate.

The photodynamic cytotoxicity of **pH-PDT** was measured as the same method. The experiment was divided into eleven groups: Control (C), laser only (L), **pH-PDT** without laser (0), and with laser for 0.5, 1.0, 1.5, 2.0, 2.5, 3.0, 3.5 and 4.0 min. Before adding MTT, cells were first seeded in 96-well plates at a density of 1×10^4 cells per well, then cultured in 5% CO_2 at 37 °C for 24 h. Cells were incubated with **pH-PDT** 1 μM for 30 min, then washed with cell culture medium. After that, cells were exposed to 532 nm laser (10 W/cm^2) for 0.5, 1.0, 1.5, 2.0, 2.5, 3.0, 3.5 and 4.0 min and incubated for another 24, 36, 48 and 60 h, respectively.

The photodynamic cytotoxicity of **pH-PDT** by AM-PI assay was also measured via CLSM imaging as the same method. The experiment was divided into eight groups: Control (C), laser only (L), **pH-PDT** without laser (0), and

with laser for 1.0, 1.5, 2.0, 2.5 and 3.0 min. HePG-2 and HL-7702 cells (5×10^8 /L) were plated on 14 mm glass coverslips and allowed to adhere for 24 h. Then the cells were incubated with **pH-PDT** (1 μM) for 2 h at 37 °C, washed with cell culture medium. After that, cells were exposed to 532 nm laser (10 W/cm^2) for 1.0, 1.5, 2.0, 2.5 and 3.0 min and incubated for another 48 h. The treated cell groups were further co-stained with 200 nM Calcine AM (AM) and 200 nM propidium iodide (PI) to distinguish live (green) and dead (red) cells for 8 min. CLSM imaging was performed on an Olympus FV1000 confocal scanning system with a 20× oil-immersion objective lens. Red channel: 617 ± 25 nm for PI (200 nM), λex = 543 nm; green channel: 515 ± 25 nm for AM (200 nM), λex = 488 nm.

Conflicts of interest

The authors declare no competing financial interest.

Acknowledgements

The authors thank for the financial support of National Natural Science Foundation of China (21671043) and National Key R&D Program of China (SQ2017YFJC020023).

Notes and references

[1] Kamkaew A, Lim SH, Lee HB, Kiew LV, Chung LY. Burgess K. BODIPY dyes in photodynamic therapy. Chem Soc Rev 2013; 42 (1): 77-88.

[2] Lucky SS, Soo KC. Zhang Y. Nanoparticles in Photodynamic Therapy. Chem Rev 2015; 115 (4): 1990-2042.

[3] Asadirad AM, Erno Z. Branda NR. Photothermal release of singlet oxygen from gold nanoparticles. Chem Commun 2013; 49 (50): 5639-5641.

[4] Zhou Z, Song J, Nie L. Chen X. Reactive oxygen species generating systems meeting challenges of photodynamic cancer therapy. Chem Soc Rev 2016; 45 (23): 6597-6626.

[5] Wilhelm S, Tavares AJ, Dai Q, Ohta S, Audet J, Dvorak HF. Chan WCW. Analysis of nanoparticle delivery to tumours. Nat Rev Mater 2016; 1: 16014.

[6] Kolemen S, Işık M, Kim GM, Kim D, Geng H, Buyuktemiz M, Karatas T, Zhang X-F, Dede Y, Yoon Jet al. Intracellular Modulation of Excited-State Dynamics in a Chromophore Dyad: Differential Enhancement of Photocytotoxicity Targeting Cancer Cells. Angew Chem Int Ed 2015; 54 (18): 5340-5344.

[7] Ichikawa Y, Kamiya M, Obata F, Miura M, Terai T, Komatsu T, Ueno T, Hanaoka K, Nagano T. Urano Y. Selective Ablation of β-Galactosidase-Expressing Cells with a Rationally Designed Activatable Photosensitizer. Angew Chem Int Ed 2014; 53 (26): 6772-6775.

[8] Chiba M, Ichikawa Y, Kamiya M, Komatsu T, Ueno T, Hanaoka K, Nagano T, Lange N. Urano Y. An Activatable Photosensitizer Targeted to γ-Glutamyltranspeptidase. Angew Chem Int Ed 2017; 56 (35): 10418-10422.

[9] Yuan Q, Wu Y, Wang J, Lu D, Zhao Z, Liu T, Zhang X. Tan W. Targeted

Bioimaging and Photodynamic Therapy Nanoplatform Using an Aptamer-Guided G-Quadruplex DNA Carrier and Near-Infrared Light. Angew Chem Int Ed 2013; 52 (52): 13965-13969.

[10] Cló E, Snyder JW, Voigt NV, Ogilby PR. Gothelf KV. DNA-Programmed Control of Photosensitized Singlet Oxygen Production. J Am Chem Soc 2006; 128 (13): 4200-4201.

[11] Park W, Park S-J, Cho S, Shin H, Jung Y-S, Lee B, Na K. Kim D-H. Intermolecular Structural Change for Thermoswitchable Polymeric Photosensitizer. J Am Chem Soc 2016; 138 (34): 10734-10737.

[12] Ozlem S. Akkaya EU. Thinking Outside the Silicon Box: Molecular AND Logic As an Additional Layer of Selectivity in Singlet Oxygen Generation for Photodynamic Therapy. J Am Chem Soc 2009; 131 (1): 48-49.

[13] Chen H, Tian J, He W. Guo Z. H_2O_2-Activatable and O_2-Evolving Nanoparticles for Highly Efficient and Selective Photodynamic Therapy against Hypoxic Tumor Cells. J Am Chem Soc 2015; 137 (4): 1539-1547.

[14] Lovell JF, Liu TWB, Chen J. Zheng G. Activatable Photosensitizers for Imaging and Therapy. Chem Rev 2010; 110 (5): 2839-2857.

[15] Kallunki T, Olsen OD. Jäättelä M. Cancer-associated lysosomal changes: friends or foes? Oncogene 2012; 32: 1995.

[16] Xue F, Wen Y, Wei P, Gao Y, Zhou Z, Xiao S. Yi T. A smart drug: a pH-responsive photothermal ablation agent for Golgi apparatus activated cancer therapy. Chem Commun 2017; 53 (48): 6424-6427.

[17] McDonnell SO, Hall MJ, Allen LT, Byrne A, Gallagher WM. O'Shea DF. Supramolecular Photonic Therapeutic Agents. J Am Chem Soc 2005; 127 (47): 16360-16361.

[18] Tian J, Ding L, Xu H-J, Shen Z, Ju H, Jia L, Bao L. Yu J-S. Cell-Specific and pH-Activatable Rubyrin-Loaded Nanoparticles for Highly Selective Near-Infrared Photodynamic Therapy against Cancer. J Am Chem Soc 2013; 135 (50): 18850-18858.

[19] Glunde K, Guggino SE, Solaiyappan M, Pathak AP, Ichikawa Y. Bhujwalla ZM. Extracellular Acidification Alters Lysosomal Trafficking in Human Breast Cancer Cells. Neoplasia 2003; 5 (6): 533-545.

[20] Montcourrier P, Mangeat PH, Valembois C, Salazar G, Sahuquet A, Duperray C. Rochefort H. Characterization of very acidic phagosomes in breast cancer cells and their association with invasion. J Cell Sci 1994; 107 (9): 2381-2391.

[21] Zhang J, Liu Z, Lian P, Qian J, Li X, Wang L, Fu W, Chen L, Wei X. Li C. Selective imaging and cancer cell death via pH switchable near-infrared fluorescence and photothermal effects. Chem Sci 2016; 7 (9): 5995-6005.

[22] Webb BA, Chimenti M, Jacobson MP. Barber DL. Dysregulated pH: a perfect storm for cancer progression. Nat Rev Cancer 2011; 11: 671.

[23] Yogo T, Urano Y, Ishitsuka Y, Maniwa F. Nagano T. Highly Efficient and Photostable Photosensitizer Based on BODIPY Chromophore. J Am Chem Soc 2005; 127 (35): 12162-12163.

[24] Qu X, Liu Q, Ji X, Chen H, Zhou Z. Shen Z. Enhancing the Stokes' shift of

BODIPY dyes via through-bond energy transfer and its application for Fe^{3+}-detection in live cell imaging. Chem Commun 2012; 48 (38): 4600-4602.

[25] Loudet A. Burgess K. BODIPY Dyes and Their Derivatives: Syntheses and Spectroscopic Properties. Chem Rev 2007; 107 (11): 4891-4932.

[26] Boens N, Leen V. Dehaen W. Fluorescent indicators based on BODIPY. Chem Soc Rev 2012; 41 (3): 1130-1172.

[27] Yang Y, Guo Q, Chen H, Zhou Z, Guo Z. Shen Z. Thienopyrrole-expanded BODIPY as a potential NIR photosensitizer for photodynamic therapy. Chem Commun 2013; 49 (38): 3940-3942.

[28] Urano Y, Asanuma D, Hama Y, Koyama Y, Barrett T, Kamiya M, Nagano T, Watanabe T, Hasegawa A, Choyke PLet al. Selective molecular imaging of viable cancer cells with pH-activatable fluorescence probes. Nat Med 2008; 15: 104.